European Journal of Radiology 74 (2010) 391–402

Contents lists available at ScienceDirect

European Journal of Radiology

journal homepage: www.elsevier.com/locate/ejrad

MRI of the brachial plexus: A pictorial review

Hendrik W. van Es*, Thomas L. Bollen, Hans P.M. van Heesewijk

Department of Radiology, St. Antonius Hospital, Nieuwegein, Koekoekslaan 1, 3435 CM Nieuwegein, The Netherlands

ARTICLE INFO

Article history:
Received 13 May 2009
Accepted 13 May 2009

Keywords:
Brachial plexus
MRI
Tumor
Trauma
Radiation therapy
Thoracic outlet syndrome

ABSTRACT

Magnetic resonance imaging (MRI) of the brachial plexus is the imaging modality of first choice for depicting anatomy and pathology of the brachial plexus. The anatomy of the roots, trunks, divisions and cords is very well depicted due to the inherent contrast differences between the nerves and the surrounding fat. In this pictorial review the technique and the anatomy will be discussed. The following pathology will be addressed: neurogenic tumors of the brachial plexus and sympathetic chain, superior sulcus tumors, other tumors in the vicinity of the brachial plexus, the differentiation between radiation and metastatic plexopathy, trauma, neurogenic thoracic outlet syndrome and immune-mediated neuropathies.

1. Introduction

Magnetic resonance imaging (MRI) is the imaging modality of first choice for depicting the anatomy and pathology of the brachial plexus [1–5]. MRI can very well demonstrate the anatomy due to its inherent contrast differences between the nerves with low signal intensity and the surrounding hyperintense fat on T1-weighted images. In this review we will discuss the normal anatomy as shown with MRI, neurogenic tumors of the brachial plexus and of the neighboring nerves, superior sulcus tumors, other tumors in the vicinity of the brachial plexus, metastatic versus radiation plexopathy, traumatic nerve root avulsion, neurogenic thoracic outlet syndrome and the immune-mediated neuropathies multifocal motor neuropathy (MMN), chronic inflammatory demyelinating polyneuropathy (CIDP) and multifocal inflammatory demyelinating neuropathy (MIDN).

2. MR technique

Our standard protocol includes sagittal T1- and T2-weighted images of the symptomatic side, coronal T1-weighted images and coronal T2-weighted images with fat suppression (T2-STIR) with thin (3 mm.) slices of both sides. Axial T1-weighted images are added in cases of superior sulcus tumors in order to evaluate the extension of the tumor towards the intervertebral foramen or vertebral body. Although oblique imaging is used [6], we prefer imaging along the straight sagittal, coronal and axial planes, as the anatomical relationships in these planes are very well known and the images can be read without specifically looking at the scanograms with scan directions. Intravenous gadolinium is administered in cases of tumor or trauma. MR-myelography is indicated to look for traumatic nerve root avulsions and pseudomeningoceles.

3. Anatomy

The brachial plexus originates from the cervical spinal nerves C5–C8 and the first thoracic spinal nerve T1. The spinal nerves split into ventral and dorsal rami just distally of the dorsal root ganglion. The dorsal rami innervate the paraspinal muscles. The five ventral rami C5, C6, C7, C8 and T1 form the brachial plexus. The ventral rami C5 and C6 join to form the upper trunk, C7 continues as the middle trunk, and the inferior trunk is formed by C8 and T1. All three trunks divide into an anterior and posterior division. The six divisions intermingle and form the three cords: the lateral, posterior and medial cord. The anterior divisions of the upper and middle trunks form the lateral cord, the anterior division of the lower trunk continues as the middle cord, and the posterior divisions of all trunks unite to form the posterior cord. At the lateral border of the pectoralis minor muscle the cords divide into the five peripheral nerves which innervate the shoulder and arm: the median, ulnar, radial, axillary and musculocutaneous nerves.

With MRI some anatomical landmarks can be used to easily identify the brachial plexus. On the sagittal images (Fig. 1) the proximal part of the first rib is used to identify the C8 and T1 nerve roots, with C8 above and T1 below the first rib (Fig. 1a). The nerve roots and the subclavian artery enter the interscalene triangle, which is formed by the anterior scalene and middle scalene muscles (Fig. 1b).

* Corresponding author.
E-mail address: h.es@antoniusziekenhuis.nl (H.W. van Es).

0720-048X/$ – see front matter © 2010 Elsevier Ireland Ltd. All rights reserved.
doi:10.1016/j.ejrad.2009.05.067

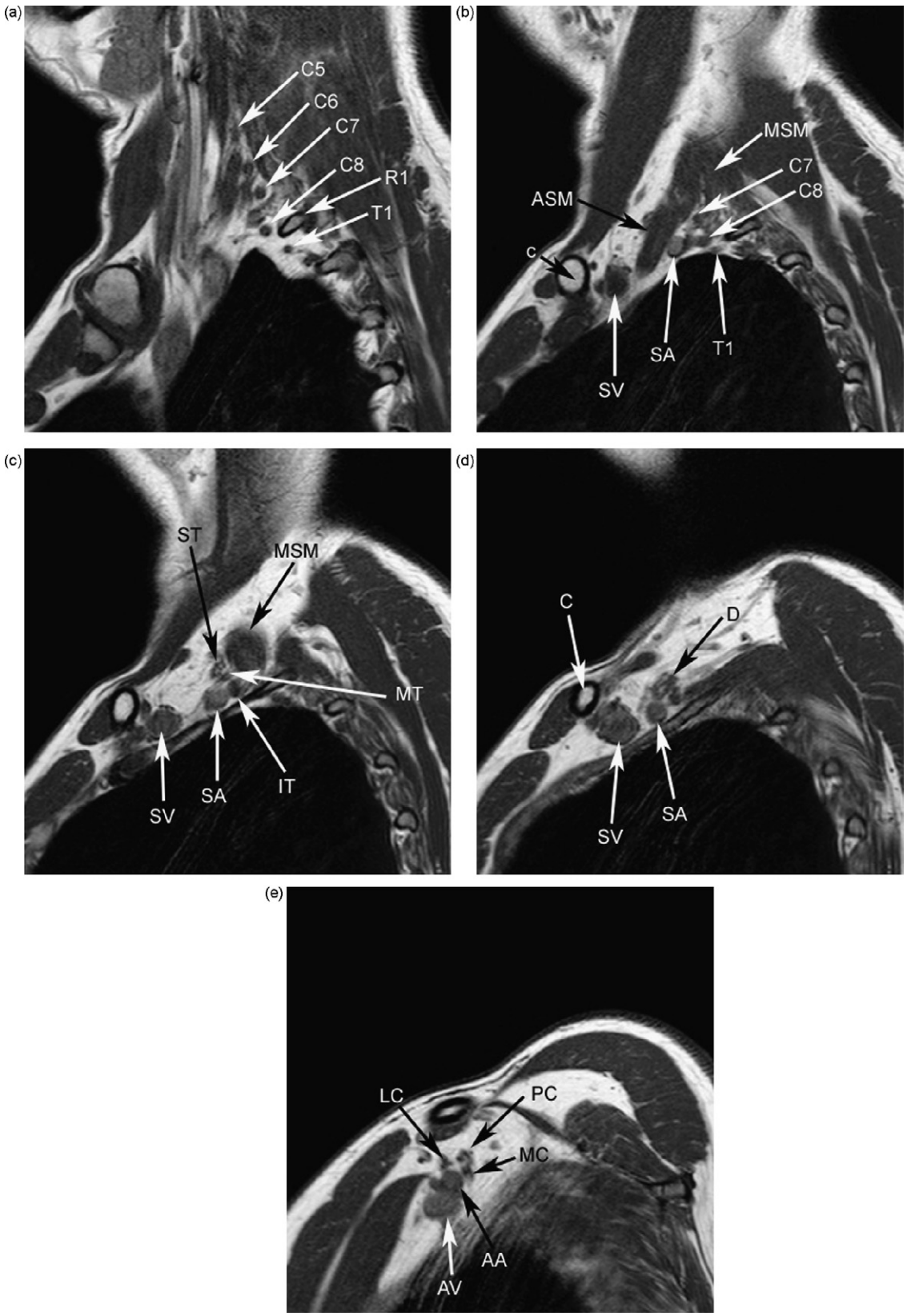

Fig. 1. Normal sagittal anatomy. (a) roots C5-T1 just lateral to the intervertebral foramina, T1 is located below and C8 above the first rib (R1). (b) Subclavian artery (SA) and the roots C7, C8 and T1 are seen within the interscalene triangle between the anterior scalene muscle (ASM) and middle scalene muscle (MSM). The subclavian vein (SV) is positioned between the anterior scalene muscle and the clavicle (c). (c) Just lateral to the interscalene triangle the three trunks are formed, the superior (ST), the middle (MT) and inferior trunk (IT). (d) The divisions (D) are formed at the level where the brachial plexus crosses the clavicle. (e) Around the axillary artery (AA) the three cords are located, the lateral (LC) most anterior, the posterior (PC) most superior and the medial (MC) most posterior. AV, axillary vein.

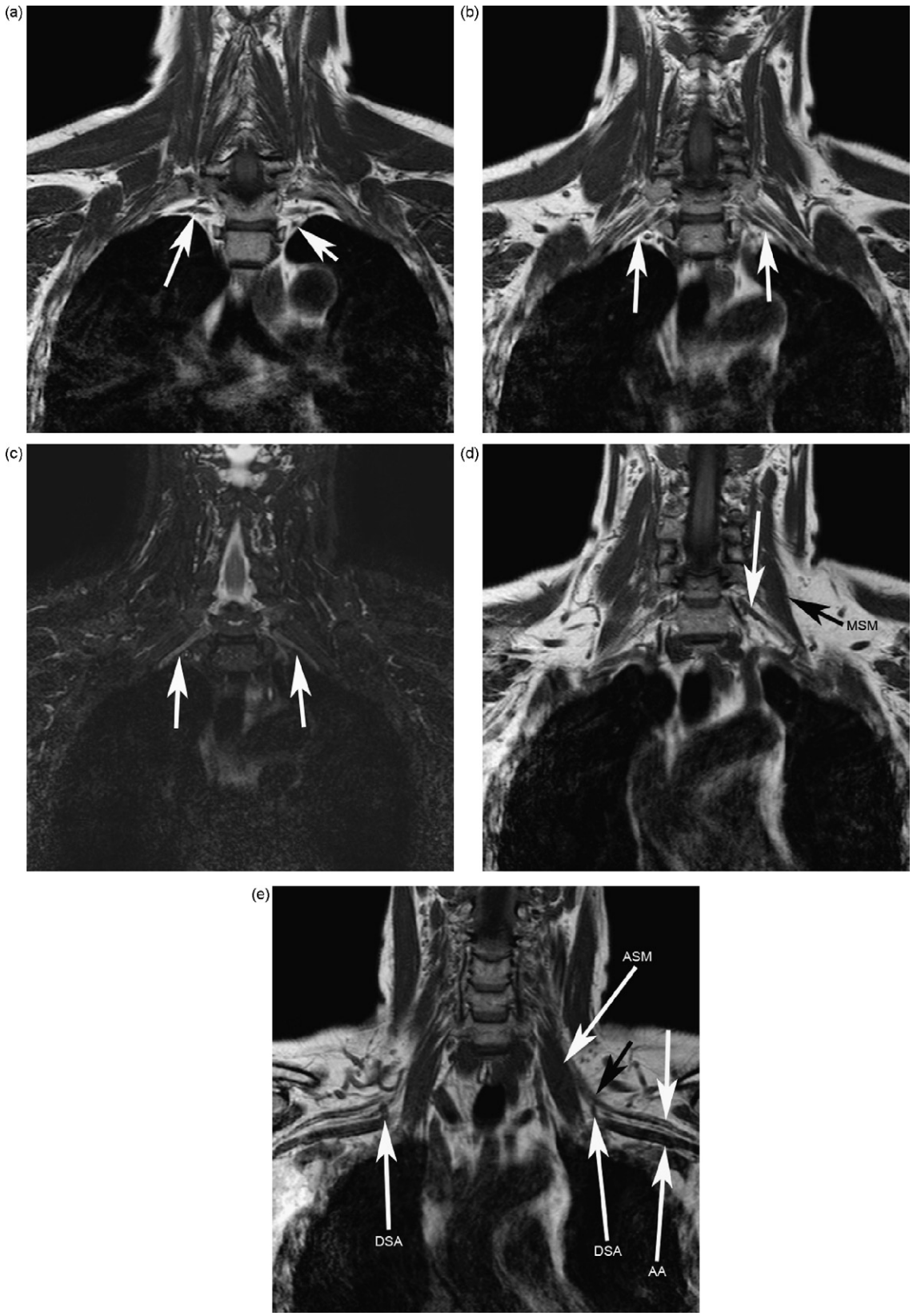

Fig. 2. Normal coronal anatomy. (a) Most posterior image with the horizontal course of the T1 nerve root (long arrow), very close to the lung apex. Short arrow points to the stellate ganglion. (b) Image just anterior to (a) with the C8 nerve roots (arrows). (c) T2-STIR image at the same level as (b) shows the slightly increased signal intensity of the normal C8 nerve roots (arrows). (d) Arrow points to the C7 nerve root. MSM, middle scalene muscle. (e) The cords (white arrow) are seen as linear structures above the axillary artery (AA). The dorsal scapular artery (DSA) courses between the trunks of the brachial plexus, black arrow points to the superior trunk. ASM, anterior scalene muscle.

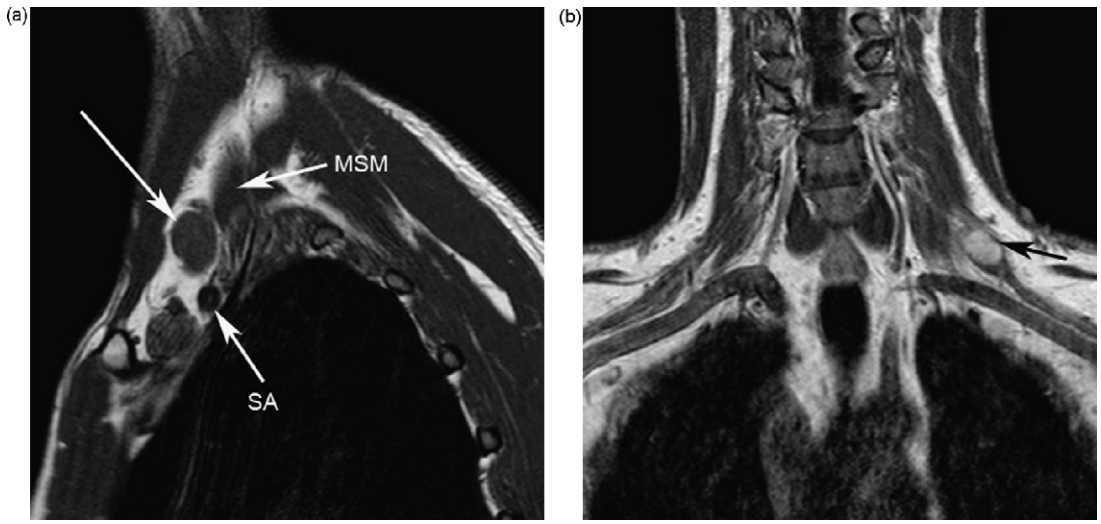

Fig. 3. Schwannoma of the superior trunk. (a) Sagittal T1-weighted image, arrow points to the tumor which is located in the superior trunk just lateral to the interscalene triangle and above the subclavian artery (SA). MSM, middle scalene muscle. (b) Coronal T1-weighted image with intravenous gadolinium shows the enhancing tumor (arrow).

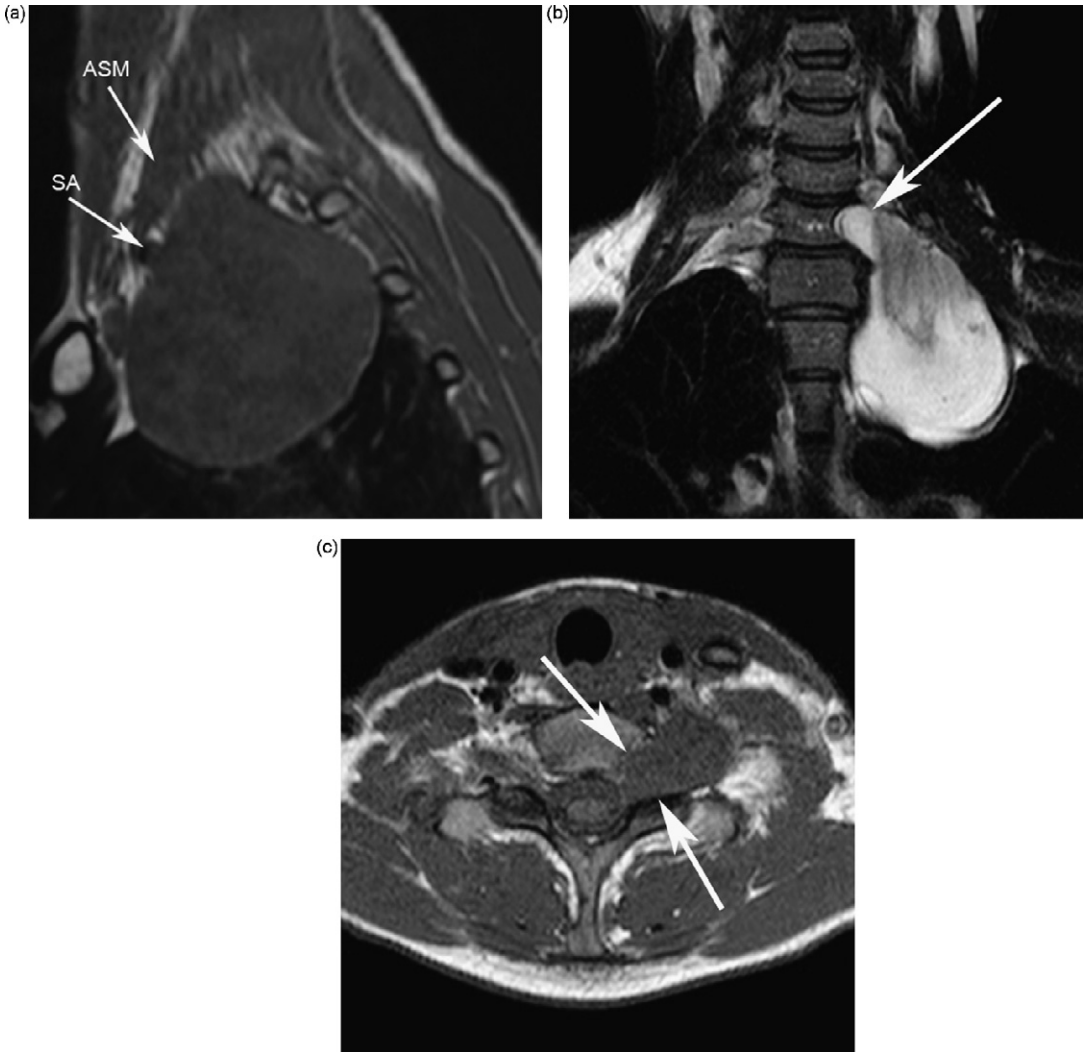

Fig. 4. Large schwannoma originating from the root C8. (a) Sagittal T1-weighted image shows the tumor in the superior sulcus and interscalene triangle. The subclavian artery (SA) and anterior scalene muscle (ASM) are displaced anteriorly. (b and c) Coronal T2-weighted image (b) and axial T1-weighted image (c) show the extension of the tumor into the intervertebral foramen C7-T1 (arrows).

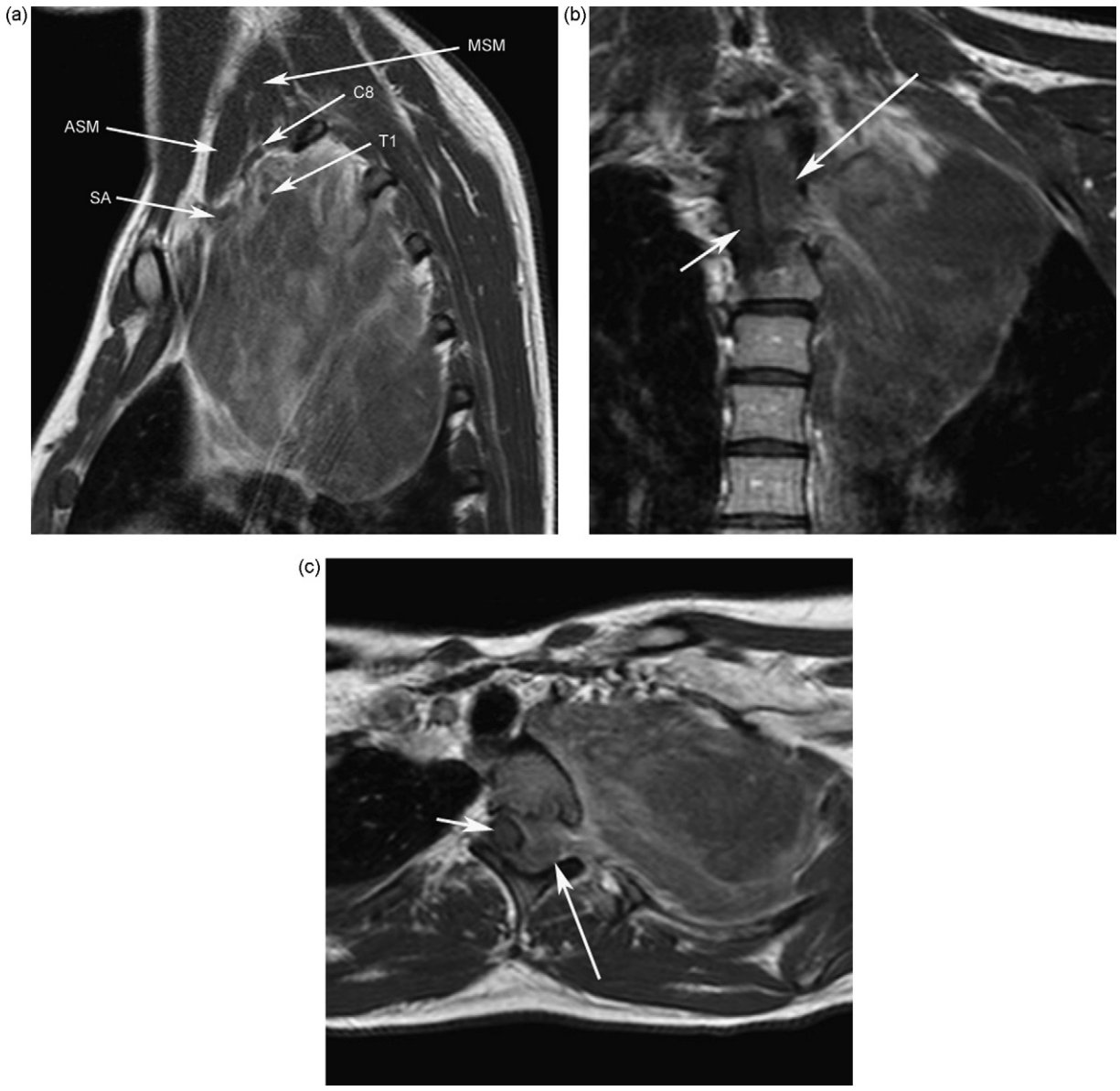

Fig. 5. Ganglioneuroma of the sympathetic chain. (a) sagittal T1-weighted image with intravenous gadolinium demonstrates an inhomogeneously enhancing tumor extending into the superior sulcus and interscalene triangle. The tumor encases root T1, and abuts root C8 and the subclavian artery (SA). ASM, anterior scalene muscle; MSM, middle scalene muscle. (b and c) Coronal (b) and axial (c) T1-weighted image with intravenous gadolinium show the extension of the tumor through the intervertebral foramen (long arrow) into the spinal canal. The spinal cord (short arrow) is shifted to the right.

Just lateral of the interscalene triangle the three trunks are formed (Fig. 1c). The divisions are located at the level where the brachial plexus crosses the clavicle (Fig. 1d). The cords are positioned above and around the axillary artery and they are named after their position relative to the axillary artery. On sagittal MRI images the lateral cord is located most anterior, the posterior cord most superior and the medial cord most posterior (Fig. 1e). On the coronal images (Fig. 2) the T1 nerve root can always be easily identified as a horizontal linear structure surrounded by fat close to the lung apex (Fig. 2a). At this level the stellate ganglion can also be identified (Fig. 2a) [7]. The C8 nerve root is also usually surrounded by fat and easily seen (Fig. 2b). On the T2-STIR images the nerves have a slightly increased signal intensity compared to the surrounding tissues (Fig. 2c) [5]. The roots C5–C7 are surrounded by less fat and have contact with the scalene muscles (Fig. 2d). To identify the trunks on the coronal images the dorsal scapular artery, a branch of the subclavian artery supplying the rhomboid muscles, can be used as a landmark (Fig. 2e). This small artery runs between the superior and middle, or middle and inferior trunk [8,9]. The subclavian and axillary artery (the subclavian artery becomes the axillary artery lateral to the lateral border of the first rib) are used as landmarks on the coronal images for the divisions and cords of the brachial plexus, as they are positioned above and around the artery.

4. Neurogenic tumors

There are four types of neurogenic tumors of the brachial plexus: schwannoma, neurofibroma, plexiform neurofibroma and malignant peripheral nerve sheath tumor (MPNST). Plexiform neurofibroma and one third of the neurofibromas are associated with neurofibromatosis type I. In patients with neurofibromatosis type I tumors are often multiple. Schwannomas have a capsule and are eccentric nerve sheath tumors. They displace the nerve fascicles and can be resected without damaging the nerve [10,11]. Neurofibromas do not have a capsule and invade the nerve fas-

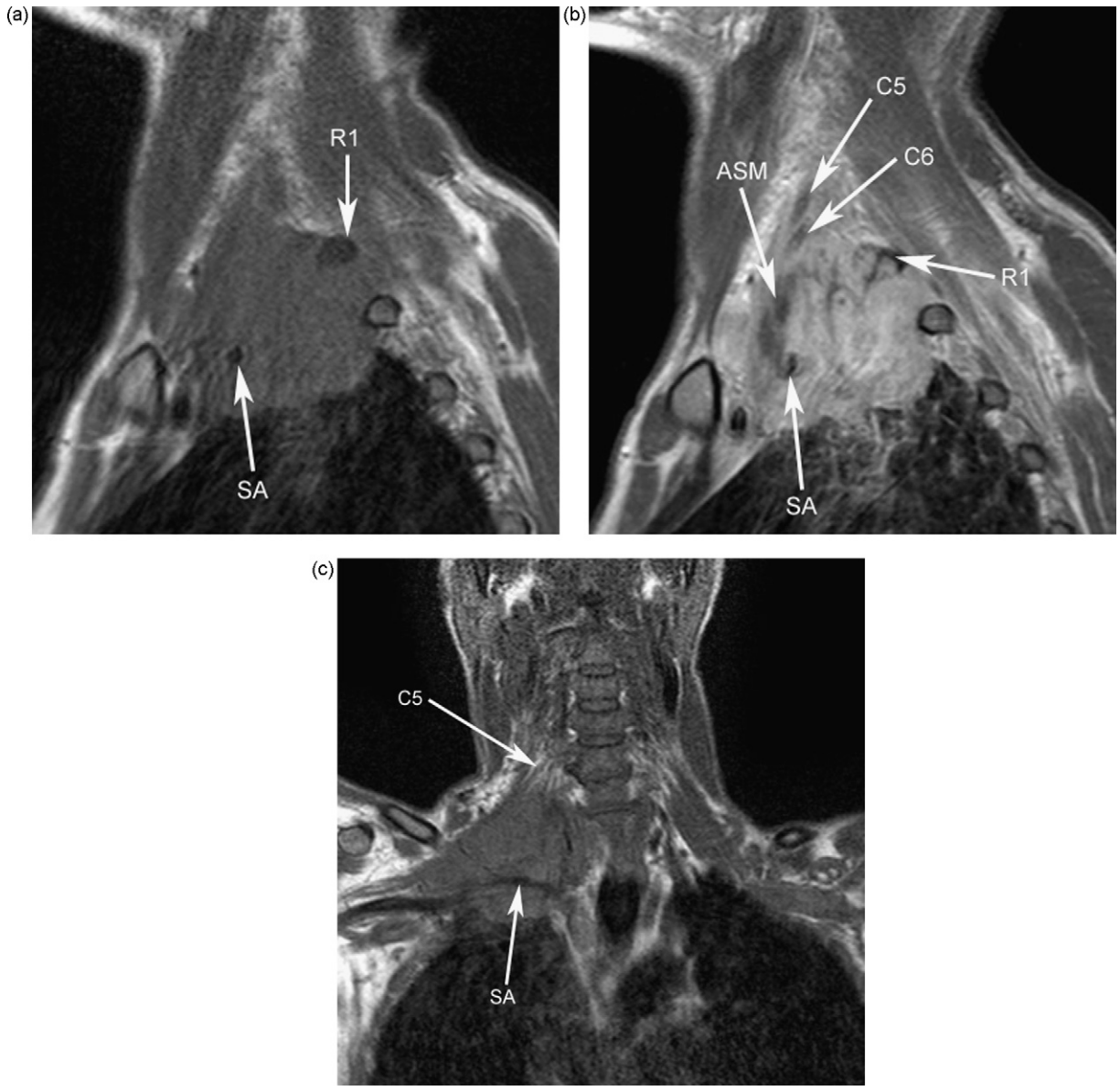

Fig. 6. Inoperable superior sulcus tumor. (a and b) Sagittal T1-weighted image without (a) and with (b) intravenous gadolinium show the extension of the non-small cell lung tumor into the interscalene triangle. With intravenous gadolinium the non-enhancing nerve roots can be discerned from the enhancing tumor, there is tumor upto the C5 nerve root. The subclavian artery (SA) is encased, the tumor surrounds the anterior scalene muscle (ASM), and there is involvement of the first rib (R1). (c) Coronal T1-weighted image demonstrates the involvement of the C5 nerve root.

cicles. Surgery without damaging the nerve is more difficult. On imaging neurogenic tumors characteristically have an ovoid form, and the nerve can often be seen entering and leaving the tumor (Fig. 3). In schwannomas the nerve enters or leaves the related tumor eccentrically, while in neurofibromas the nerve passes through the center of the tumor [12]. These tumors have signal intensity similar to muscle on T1-weighted images and markedly increased signal intensity on T2-weighted images. They enhance with intravenous gadolinium. Cystic parts may be present in schwannomas. Neurogenic tumors may present as an apical lung tumor (Fig. 4) [3]. MPNST's cannot reliably be differentiated by imaging alone, although there are some features which may suggest malignancy, such as poorly defined margins and bone destruction [12].

Neurogenic tumors of nerves in the vicinity of the brachial plexus include those of the vagal nerve, phrenic nerve and sympathetic trunk. The course of those tumors is in a more vertical direction [12]. Tumors of the sympathetic chain can also have a ganglion cell origin: neuroblastoma, ganglioneuroblastoma and ganglioneuroma (Fig. 5).

5. Superior sulcus tumors

Superior sulcus tumors are non-small cell lung carcinomas that arise from the lung apex and invade the thoracic inlet [13]. The term superior sulcus has been described by Pancoast [14] and he presumably meant the groove of the subclavian artery in the pleural cuff [15]. Pancoast suggested that the origin of the tumor is an embryonic rest of the fifth pharyngeal pouch in the superior pulmonary sulcus, however in 1932 Tobias, an Argentine physician described the true nature of these tumors: the lung [16]. Classically patients present with Pancoast's syndrome which includes pain in the shoulder and arm, weakness and atrophy of the muscles of the hand, and Horner's syndrome. Tumor infiltration of the stellate ganglion causes Horner's syndrome, which is characterized by miosis,

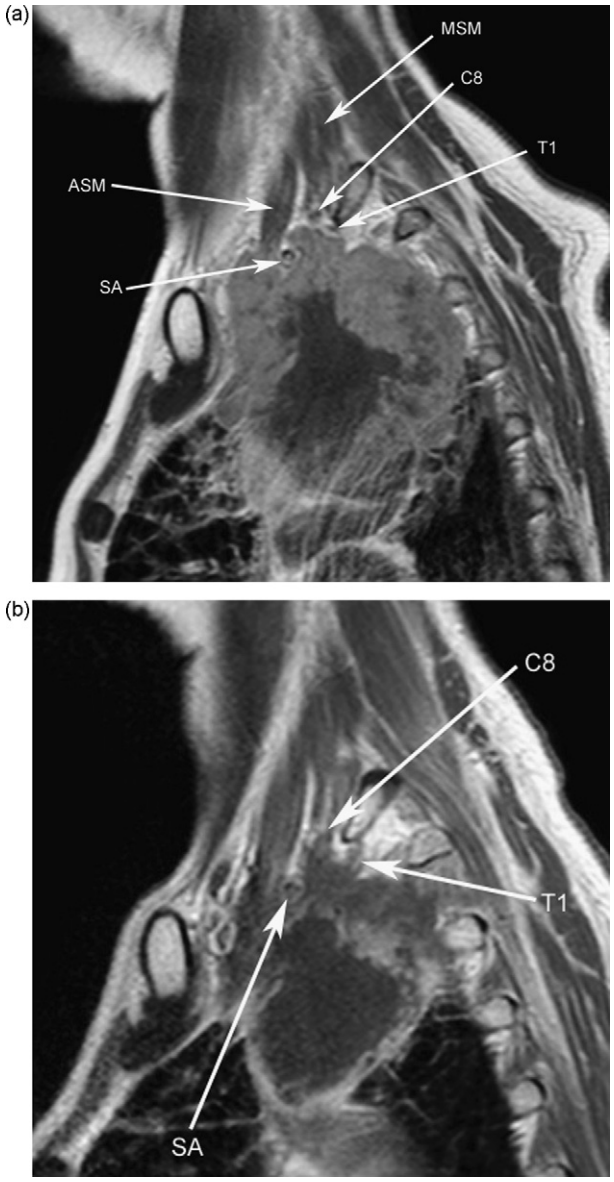

Fig. 7. Operable superior sulcus tumor. (a) Sagittal T1-weighted image with intravenous gadolinium pre chemo- and radiation therapy shows the invasion of the non-small cell lung carcinoma into the interscalene triangle between the anterior (ASM) and middle scalene (MSM) muscle. The tumor abuts the roots C8 and T1, and the subclavian artery (SA). (b) Sagittal T1-weighted image with intravenous gadolinium post chemo- and radiation therapy demonstrates the shrinkage of the tumor, especially of the enhancing rim. However the invasion into the interscalene triangle has not changed much, the tumor abuts the roots C8 and T1, and the subclavian artery. At curative surgery only scar tissue was found in the interscalene triangle, so that the roots of C8 and T1 could be spared.

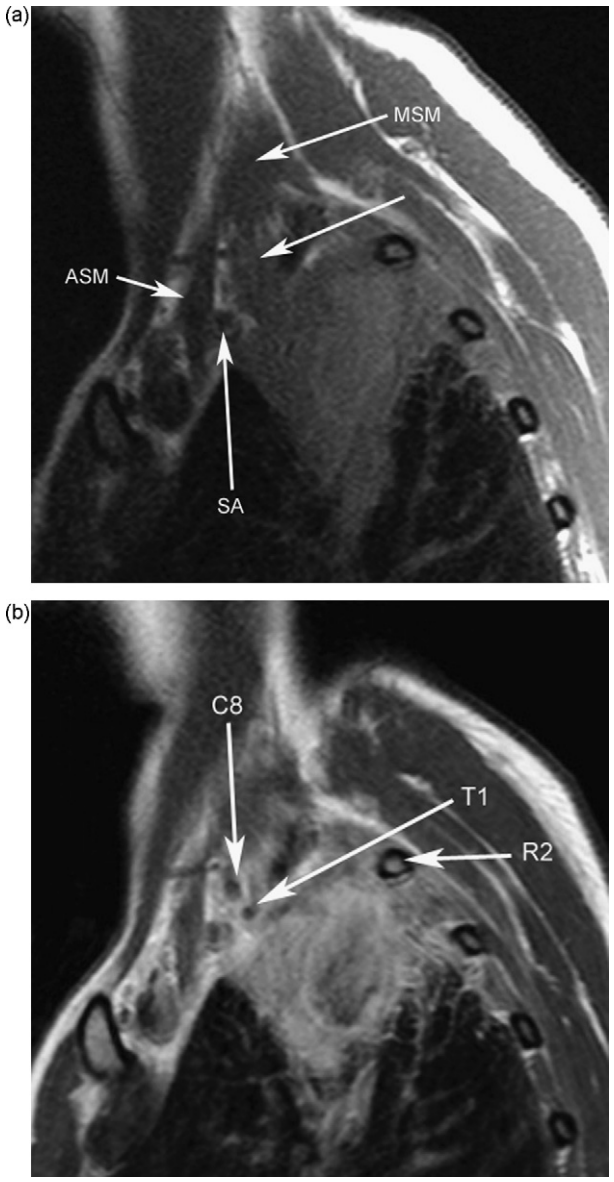

Fig. 8. Nocardia infection in the superior sulcus. a and b: sagittal T1-weighted image without (a) and with (b) intravenous gadolinium show an enhancing mass in the superior sulcus with interscalene triangle invasion (arrow in a). The mass surrounds the C8 and T1 nerve roots. There is involvement of the enhancing second rib (R2). Surgical biopsy revealed that this mass, which mimics a super sulcus lung tumor, was a nocardia infection. SA, subclavian artery; ASM, anterior scalene muscle; MSM, middle scalene muscle.

ptosis and anhidrosis. MRI is very useful to examine local tumor extension towards the brachial plexus, vertebral bodies, intervertebral foramina and the subclavian vessels. Contra-indications for surgery include brachial plexus involvement above C8 (Fig. 6), vertebral body invasion of more than 50% and extensive mediastinal involvement with invasion of esophagus or trachea [17,18]. At our institution the standard therapy is pre-operative chemoradiation therapy after which a new MRI is performed. In our experience the remaining enhancing tissue is sometimes only reactive fibrous tissue secondary to chemoradiation therapy without viable tumor cells (Fig. 7). In those cases it is possible to release nerves that are located at the border of these tissues. Peroperative biopsies should be obtained in order to determine whether sacrificing parts of the brachial plexus is necessary [19].

Infection may radiographically mimic a malignant superior sulcus tumor. Especially Nocardia is known to invade the thoracic wall (Fig. 8) [20].

6. Other tumors in the vicinity of the brachial plexus

In this category metastatic disease is the most common cause, especially metastases from lung and breast carcinoma. MRI can very well depict the relationship of these tumors with the brachial plexus (Fig. 9).

Other tumors include benign and malignant soft tissue tumors, bone tumors and metastatic disease [4]. The most common benign soft tissue tumors that may involve the brachial plexus are lipoma (Fig. 10) and aggressive fibromatosis. Although histologically benign, aggressive fibromatosis is difficult to resect completely and has a tendency to recur [21,22]. Malignant soft tis-

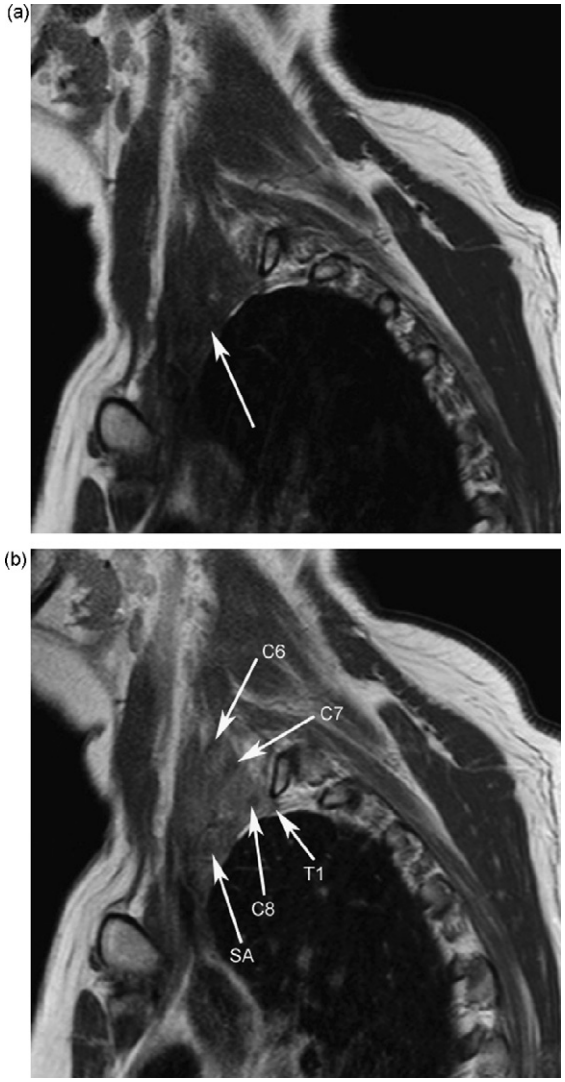

Fig. 9. Metastasis of breast carcinoma in the interscalene triangle with involvement of the brachial plexus. (a and b) Sagittal T1-weighted image without (a) and with (b) intravenous gadolinium demonstrate the obliterated fat in the interscalene triangle (arrow in a). Only after contrast administration the involved nerve roots C6, C7, C8, T1 and the subclavian artery (SA) can be discerned.

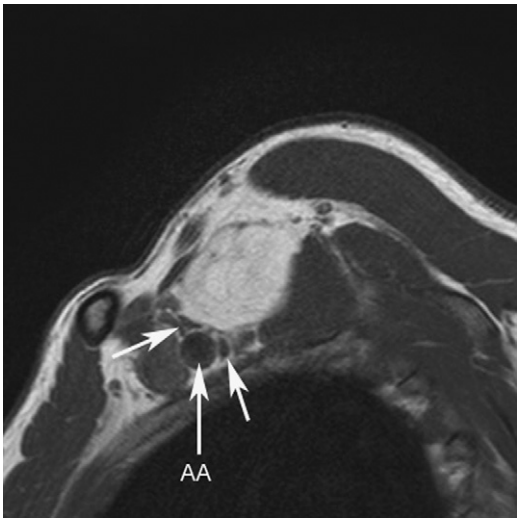

Fig. 10. Sagittal T1-weighted image of a lipoma with mass effect on the brachial plexus (arrows). AA, axillary artery.

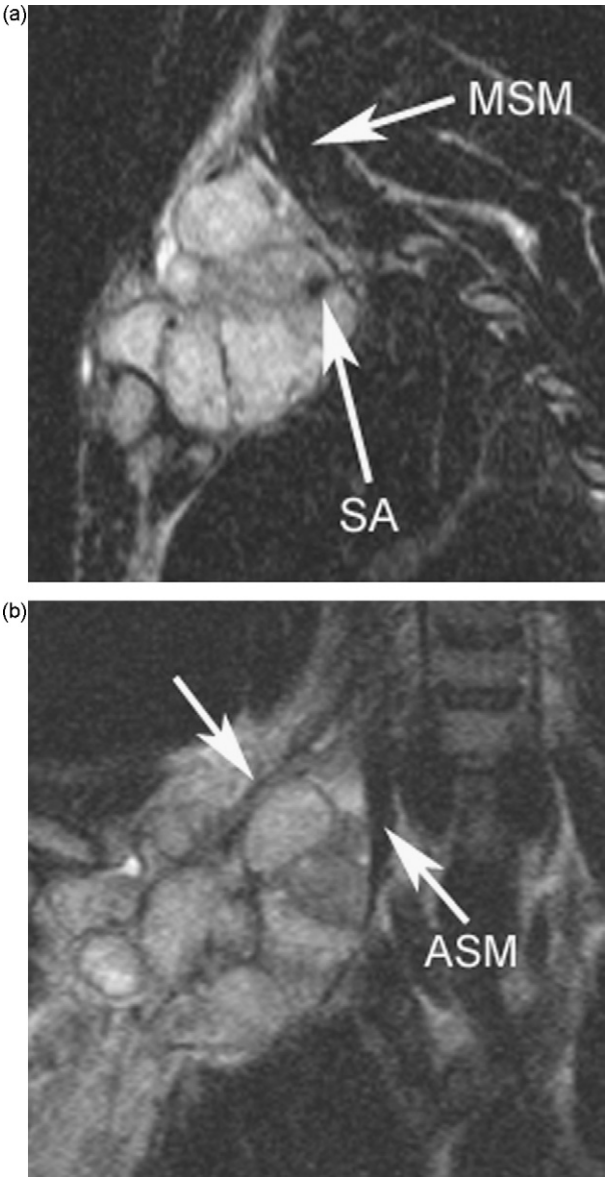

Fig. 11. Synovial cell sarcoma. (a) sagittal T2-weighted image shows the hyperintense mass with encasement of the subclavian artery (SA). MSM, middle scalene muscle. (b) Coronal T2-weighted image demonstrates the encasement of the upper brachial plexus (arrow) and the medial displacement of the anterior scalene muscle (ASM).

sue tumors include various types of sarcomas, such as liposarcoma, leiomyosarcoma, malignant fibrous histiocytoma and synovial cell sarcoma (Fig. 11).

All kind of bone tumors of the first rib, clavicle, scapula and vertebral bodies may involve the brachial plexus. In this group bone metastases are the most common cause; other rare causes include plasmocytoma, chondrosarcoma and osteochondroma.

7. Metastatic versus radiation plexopathy

The most common source of metastatic disease that can cause brachial plexopathy is breast carcinoma. Other metastases include those from lung carcinoma and head and neck cancer. Especially in patients with a history of breast cancer and who have been treated with radiation therapy the clinical distinction between neoplastic brachial plexopathy and radiation plexopathy may be difficult. Some signs and symptoms may be useful. Horner's syndrome, lower

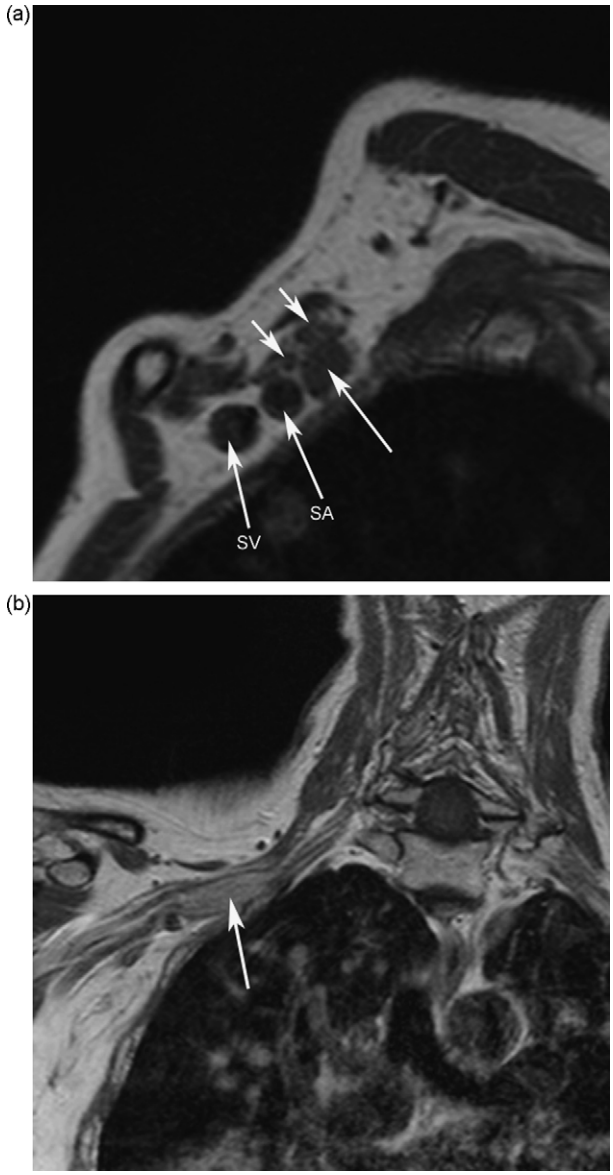

Fig. 12. Metastatic plexopathy of breast carcinoma. (a) Sagittal T1-weighted image shows a mass at the level of the divisions of the brachial plexus (long arrow). Note the normal neighboring nerves of the brachial plexus (short arrows). SA, subclavian artery; SV, subclavian vein. (b) Coronal T1-weighted image with intravenous gadolinium demonstrates the enhancement of the metastasis (arrow).

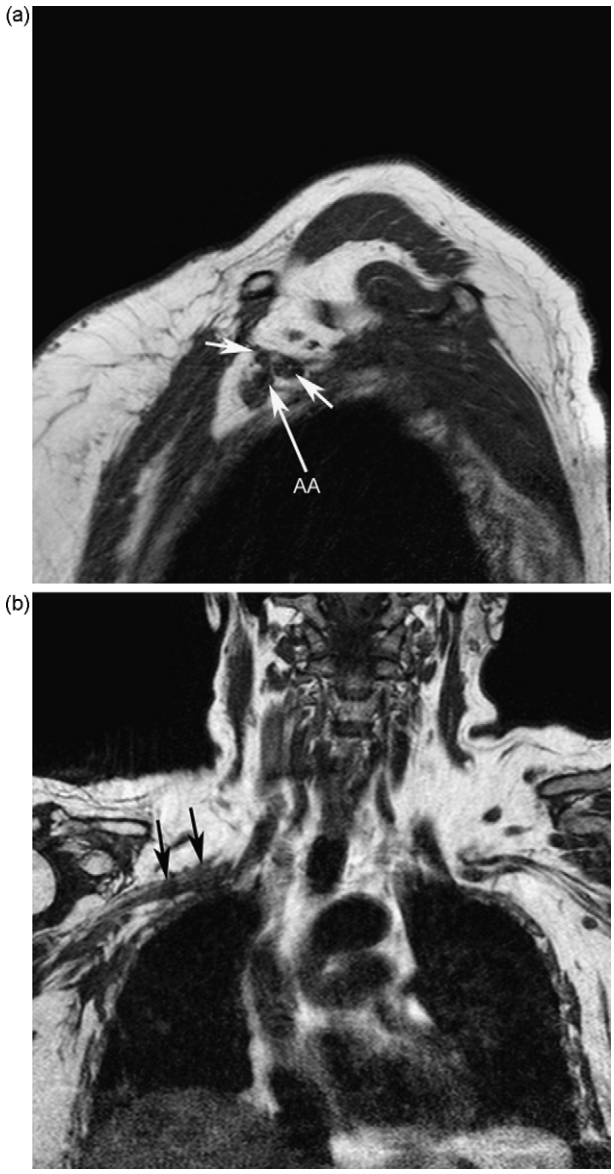

Fig. 13. Radiation plexopathy of breast carcinoma. (a) Sagittal T1-weighted image shows diffuse thickening of the cords (arrows), which cannot be discerned separately. AA, axillary artery. (b) Coronal T1-weighted image shows diffuse thickening of the brachial plexus (arrows) compared to the normal left side.

(C7, C8 and T1) brachial plexus involvement, severe pain, hand weakness and a latency period of more than 1 year suggest tumor infiltration. Upper (C5 and C6) brachial plexus involvement, no pain, lymphedema and a latency period of less than 1 year are consistent with radiation-induced brachial plexopathy [23]. MRI is very helpful in making this differentiation. Radiation fibrosis is usually low on T1- and T2-weighted images and does not enhance after the administration of intravenous gadolinium. However fibrosis can have high signal intensity on T2-weighted images and may enhance [24]. Tumor characteristically is low on T1- and high on T2-weighted images and enhances with contrast. However, the signal intensity characteristics of tumor can be variable [25]. The most useful sign of tumor on MRI is the presence of a focal mass (Fig. 12) [25]. Radiation fibrosis usually causes an architectural distortion and a more diffuse thickening of the brachial plexus without a focal mass (Fig. 13).

8. Traumatic nerve root avulsion

Traumatic brachial plexus lesions in adults are often caused by high-energy accidents, such as motorcycle accidents. It is important to differentiate between pre- and postganglionic injuries, which is clinically difficult. This is crucial for surgical management and prognosis. The prognosis is better in postganglionic injuries, where surgical repair in the form of nerve grafting is possible. In preganglionic injuries, usually nerve root avulsions, direct surgical repair cannot be done. Function can only be restored by neurotization techniques, in which a nerve is moved to another end organ, or musculotendinous transpositions.

MRI of postganglionic injuries can show thickened nerves with a low signal intensity on T1-weighted images and an increased signal intensity on T2-weighted images. Nerve contiguity can be seen, or there can be discontinuity with distal nerve contraction [6]. Direct brachial plexus compression by a hematoma, fracture fragment or callus formation can also cause brachial plexopathy [2]. MRI of preganglionic injuries can show nerve

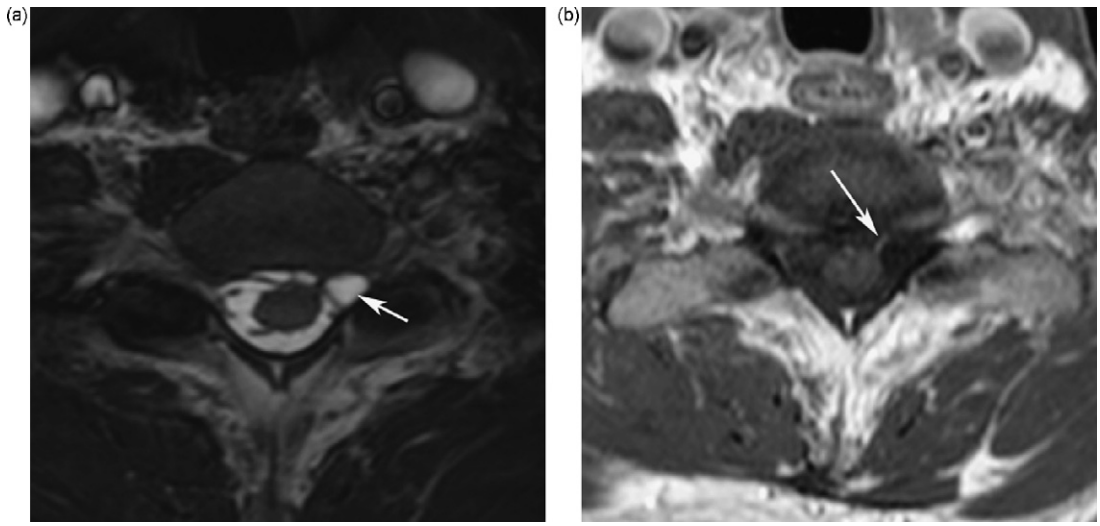

Fig. 14. Traumatic nerve root avulsion. (a) Axial balanced-FFE image demonstrates a traumatic pseudomeningocele (arrow). (b) Axial T1-weighted image with intravenous gadolinium shows the enhancement of an avulsed nerve root (arrow).

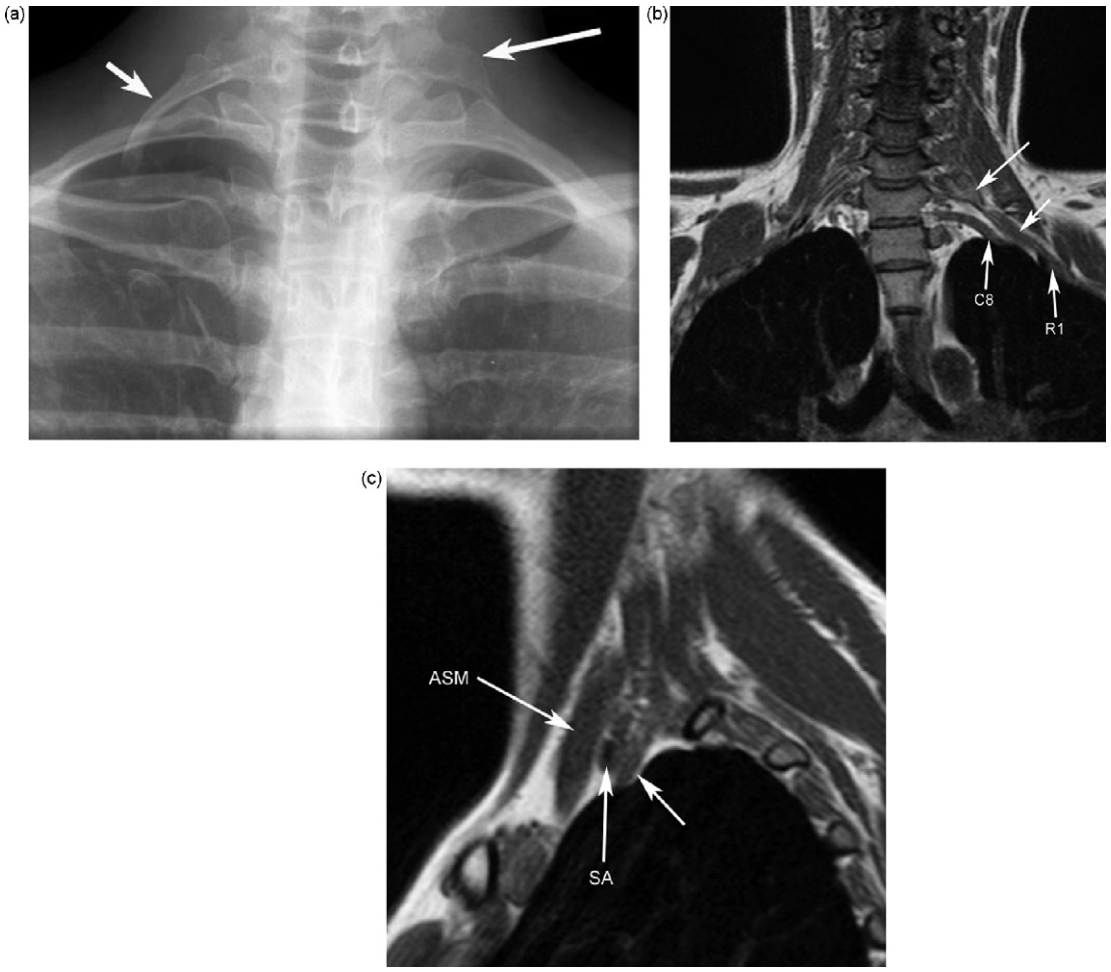

Fig. 15. Left-sided neurogenic thoracic outlet syndrome. (a) Radiograph shows a cervical rib on the asymptomatic side (small arrow) and a hypertrophic transverse process of C7 on the symptomatic side (long arrow). (b) Coronal T1-weighted image demonstrates that the fibrous band (short arrow), which courses from the hypertrophic transverse process of C7 (long arrow) to the first rib (R1), causes a deviation of the C8 nerve root. (c) Sagittal T1-weighted shows the fibrous band (arrow) within the interscalene triangle. SA, subclavian artery; ASM, anterior scalene muscle.

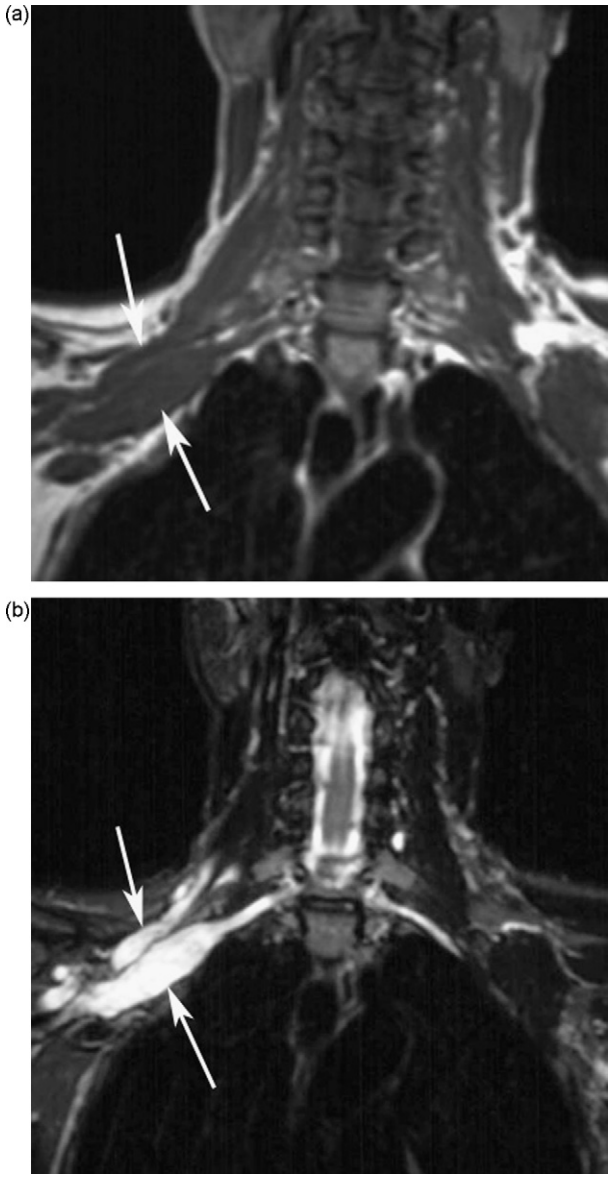

Fig. 16. MIDN (a and b) coronal T1-weighted (a) and T2-STIR (b) image show thickening of the brachial plexus (arrows) with an increased signal intensity on the T2-weighted images.

root avulsions with or without pseudomeningoceles (Fig. 14a). Pseudomeningoceles are cerebrospinal fluid collections due to a dural tear. The presence of a pseudomeningocele is a valuable but not pathognomonic sign for a preganglionic lesion, as pseudomeningoceles can occur without nerve root avulsions, and nerve root avulsions not always coincide with pseudomeningoceles. Spinal cord abnormalities occur in 20% with preganglionic injuries, such as edema, hemorrhage and myelomalacia [26]. Administration of intravenous gadolinium can be useful in diagnosing preganglionic injuries. An uncommon but useful finding is the enhancement of intradural nerve roots or root stumps (Fig. 14b), which indicates functional impairment [26,27]. An explanation can be the breakdown of the blood-nerve barrier or dilatation of radicular veins. Enhancement of denervated paraspinal muscles, especially the multifidus muscle, is another sign of nerve root avulsion [26,28]. Dilatation of the vascular bed and enlargement of the extracellular space cause this abnormal enhancement.

9. Neurogenic thoracic outlet syndrome

Neurogenic thoracic outlet syndrome occurs in young women. It has characteristic electrophysiological characteristics and typical clinical features, such as hand weakness and wasting of the lateral thenar muscles [29]. Radiography of the neck shows congenital bony abnormalities, consisting of a rudimentary cervical rib or an elongated transverse process of C7, which should not be larger than the transverse process of T1 (Fig. 15a). In these patients a fibrous band runs from the elongated transverse process or rudimentary cervical rib to the first rib which gives compression on the nerve roots C8 or T1 or the inferior trunk. MRI can be helpful in showing the fibrous band and an asymmetry in the course of lower brachial plexus (Fig. 15b and c) [30–32].

10. Immune-mediated neuropathies: MMN, CIDP and MIDN

MMN is characterized by slowly progressive, asymmetrical weakness of the limbs without sensory loss. CIDP causes a symmetrical weakness of the limbs with sensory loss [33]. Patients with MIDN have an asymmetrical sensory loss with or without weakness [34]. These immune-mediated neuropathies can be treated with intravenous immunoglobulins. Electrophysiological studies are often diagnostic. MRI of the affected peripheral nerves can be abnormal. The nerves are enlarged and have an increased signal intensity on T2-weighted images (Fig. 16). T2-weighted images with fat suppression are very useful in these patients. The lesions may, but often do not enhance after the administration of intravenous gadolinium. The abnormalities on MRI may mimic hereditary motor-sensory neuropathy (synonyms: hypertrophic neuropathy or Charcot–Marie-Tooth syndrome) or plexiform neurofibromatosis [6]. The clinical differentiation between MMN and lower motor neuron disease can be clinically difficult. In these cases MRI of the brachial plexus can be helpful, as the brachial plexus is normal in patients with lower motor neuron disease [35].

References

[1] Bowen BC, Seidenwurm DJ. Plexopathy. AJNR Am J Neuroradiol 2008;29:400–2.
[2] Van Es HW. MRI of the brachial plexus. Eur Radiol 2001;11:325–36.
[3] Todd M, Shah GV, Mukherji SK. MR imaging of brachial plexus. Top Magn Reson Imaging 2004;15:113–25.
[4] Wittenberg KH, Adkins MC. MR imaging of nontraumatic brachial plexopathies: frequency and spectrum of findings. Radiographics 2000;20:1023–32.
[5] Bowen BC, Pattany PM, Saraf-Lavi E, Maravilla KR. The brachial plexus: normal anatomy, pathology, and MR imaging. Neuroimaging Clin N Am 2004;14:59–85.
[6] Sureka J, Cherian RA, Alexander M, Thomas BP. MRI of brachial plexopathies. Clin Radiol 2009;64:208–18.
[7] Hogan QH, Erickson SJ. MR imaging of the stellate ganglion: normal appearance. AJR Am J Roentgenol 1992;158:655–9.
[8] Van Es HW, Witkamp TD, Feldberg MAM. MRI of the brachial plexus and its region: anatomy and pathology. Eur Radiol 1995;5:145–51.
[9] Demondion X, Boutry N, Drizenko A, Paul C, Francke JP, Cotten A. Thoracic outlet: anatomic correlation with MR imaging. AJR Am J Roentgenol 2000;175:417–22.
[10] Lusk MD, Kline DG, Garcia CA. Tumors of the brachial plexus. Neurosurgery 1987;21:439–53.
[11] Sell PJ, Semple JC. Primary nerve tumours of the brachial plexus. Br J Surg 1987;74:73–4.
[12] Saifuddin A. Imaging tumours of the brachial plexus. Skelet Radiol 2003;32:375–87.
[13] Bruzzi JF, Komaki R, Walsh GL, et al. Imaging of non-small cell lung cancer of the superior sulcus: part 1: anatomy, clinical manifestations, and management. Radiographics 2008;28:551–60.
[14] Pancoast HK. Superior pulmonary sulcus tumor: tumor characterized by pain. Horner's syndrome, destruction of bone and atrophy of hand muscles. JAMA 1932;99:1391–6.
[15] Hepper NGG, Herskovic T, Witten DM, Mulder DW, Woolner LB. Thoracic inlet tumors. Ann Intern Med 1966;64:979–89.
[16] Tobias JW. Syndrome apico-costo-vertebral doloroso por tumor, apexiano: su valor diagnostico en el cancer primitivo pulmonar. Rev Med Lat Am 1932;17:1522–666.

[17] Dartevelle PG, Macchiarini P. Surgical management of superior sulcus tumors. Oncologist 1999;4:398–407.
[18] Bruzzi JF, Komaki R, Walsh GL, et al. Imaging of non-small cell lung cancer of the superior sulcus: part 2: initial staging and assessment of resectability and therapeutic response. Radiographics 2008;28:561–72.
[19] Bilsky MH, Vitaz TW, Boland PJ, Bains MS, Rajaraman V, Rusch VW. Surgical treatment of superior sulcus tumors with spinal and brachial plexus involvement. J Neurosurg Spine 2002;97:301–9.
[20] Yoon HK, Im JG, Ahn JM, Han MC. Pulmonary nocardiosis: CT findings. J Comput Assist Tomogr 1995;19:52–5.
[21] Garant M, Just N. Aggressive fibromatosis of the neck: MR findings. AJNR Am J Neuroradiol 1997;18:1429–31.
[22] Lee JC, Thomas JM, Phillips S, Fisher C, Moskovic E. Aggressive fibromatosis: MRI features with pathologic correlation. AJR Am J Roentgenol 2006;186: 247–54.
[23] Kori SH, Foley KM, Posner JB. Brachial plexus lesions in patients with cancer: 100 cases. Neurology 1981;31:45–50.
[24] Van Es HW, Engelen AM, Witkamp TD, Ramos LMP, Feldberg MAM. Radiation-induced brachial plexopathy: MR imaging. Skelet Radiol 1997;26:284–8.
[25] Qayyum A, MacVicar AD, Padhani AR, Revell P, Husband JE. Symptomatic brachial plexopathy following treatment for breast cancer: utility of MR imaging with surface-coil techniques. Radiology 2000;214:837–42.
[26] Yoshikawa T, Hayashi N, Yamamoto S, et al. Brachial plexus injury: clinical manifestations. conventional imaging findings, and the latest imaging techniques. Radiographics 2006;26:S133–43.
[27] Hayashi N, Yamamoto S, Okubo T, et al. Avulsion injury of cervical nerve roots: enhanced intradural nerve roots at MR imaging. Radiology 1998;206:817–22.
[28] Hayashi N, Masumoto T, Abe O, Aoki S, Ohtomo K, Tajiri Y. Accuracy of abnormal paraspinal muscle findings on contrast-enhanced MR images as indirect signs of unilateral cervical root-avulsion injury. Radiology 2002;223:397–402.
[29] Tilki HE, Stalberg E, Incesu L, Basoglu A. Bilateral neurogenic thoracic outlet syndrome. Muscle Nerve 2004;29:147–50.
[30] Panegyres PK, Moore N, Gibson R, Rushworth G, Donaghy M. Thoracic outlet syndromes and magnetic resonance imaging. Brain 1993;116:823–41.
[31] Demondion X, Bacqueville E, Paul C, Duquesnoy B, Hachulla E, Cotten A. Thoracic outlet: assessment with MR imaging in asymptomatic and symptomatic populations. Radiology 2003;227:461–8.
[32] Demondion X, Herbinet P, Van Sint JS, Boutry N, Chantelot C, Cotten A. Imaging assessment of thoracic outlet syndrome. Radiographics 2006;26: 1735–50.
[33] Van den Berg LH, Franssen H, Van Asseldonk JT, Van Den Berg-Vos RM, Wokke JH. Chapter 12 multifocal and other motor neuropathies. Handb Clin Neurol 2007;82:229–45.
[34] Van den Berg-Vos RM, van den Berg LH, Franssen H, et al. Multifocal inflammatory demyelinating neuropathy: a distinct clinical entity? Neurology 2000;54:26–32.
[35] Van Es HW, van den Berg LH, Franssen H, et al. Magnetic resonance imaging of the brachial plexus in patients with multifocal motor neuropathy. Neurology 1997;48:1218–24.